Available online at www.sciencedirect.com
ScienceDirect
European Journal of Medicinal Chemistry 42 (2007) 627–634
EUROPEAN JOURNAL OF MEDICINAL CHEMISTRY
http://www.elsevier.com/locate/ejmech

Original article

Metal complexes of retinoid derivatives with antiproliferative activity: Synthesis, characterization and DNA interaction studies

F. Bisceglie [a,*], M. Baldini [a], M. Belicchi-Ferrari [a], E. Buluggiu [b], M. Careri [a], G. Pelosi [a], S. Pinelli [c], P. Tarasconi [a]

[a] *Dipartimento di Chimica Generale ed Inorganica, Chimica Analitica, Chimica Fisica, Viale G. P. Usberti 17/A, Campus Universitario, Università degli Studi di Parma, 43100 Parma, Italy*
[b] *Dipartimento di Sanità Pubblica – Sezione di Fisica – Via Volturno 39, Università degli Studi di Parma, 43100 Parma, Italy*
[c] *Dipartimento di Clinica Medica, Nefrologia e Scienze della Prevenzione, Via Gramsci 14, Università degli Studi di Parma, 43100 Parma, Italy*

Received 20 September 2006; received in revised form 29 November 2006; accepted 5 December 2006
Available online 12 January 2007

Abstract

9-*cis*-Retinal thiosemicarbazone and its Co(III), Ni(II) and Cu(II) complexes are synthesized and characterized. Central Co(III) atom is in an octahedral environment while Ni(II) and Cu(II) atoms are in a square planar environment. DNA binding constants and spectroscopic data show an intercalative behavior for the nickel complex; an external binding mode is envisaged for the ligand and its copper complex. No DNA interaction can be hypothesized for the cobalt complex. The free ligand and its Ni(II) and Cu(II) complexes have a good lipophilic degree for an efficient uptake by the cells. The metal complexes exhibit a proliferation inhibition action against cell line U937 at micromolar concentration. Cu(II) complex also induces apoptosis, while Ni(II) complex has a strong interaction with CT-DNA.

Keywords: Thiosemicarbazones; Retinoids; Metal complexes; DNA; U937

1. Introduction

Thiosemicarbazones are a class of compounds of medical applicative interest. Many of them, such as Marboran® or Triapine™, have been used and are still in the clinical practice [1]. Thiosemicarbazones are promising in the treatment of many diseases, cancer amongst all, and their development is still in progress [2–5]. Following our interest in the field of natural aldehyde thiosemicarbazone metal complexes [6,7], we decided to focus our attention on retinal because retinoids are very interesting class of compounds really promising as chemotherapic drugs [8–11] and at present it seems useful to use a combined therapy between retinoids and other drugs or drugs derived from retinoids in order to overcome their limits of chemoresistance and toxicity [9]. In addition, to our knowledge no metal complexes of retinoid derivatives have been evaluated as chemotherapic agents.

With these requirements a new ligand derived from 9-*cis*-retinal and thiosemicarbazide, Hret (**1**) (see Scheme 1), has been synthesized and fully characterized.

Three metal complexes $[Cu(ret)Cl(OH_2)]\cdot H_2O$ (**2**), $[Co(Hret)_3]Cl_3\cdot 4H_2O$ (**3**), and $[Ni(ret)_2]\cdot 3H_2O$ (**4**) have therefore been synthesized and characterized by means of spectroscopy (IR, UV, NMR, ESR, ESI-MS) and elemental analysis. Cu(II), Ni(II) and Co(III) metal ions have been chosen because we already observed that these ions enhance thiosemicarbazones' biological activity [7]. Moreover, as small molecules, these compounds can react at specific sites along a DNA strand through a series of weak interactions [12] allowing the metal center to approach the nucleic acid and to interact with it. To quantify the DNA binding capability in aqueous solution,

* Corresponding author. Tel.: +39 0521 905420; fax: +39 0521 905557.
E-mail address: franco.bisceglie@unipr.it (F. Bisceglie).

0223-5234/$ - see front matter © 2007 Elsevier Masson SAS. All rights reserved.
doi:10.1016/j.ejmech.2006.12.019

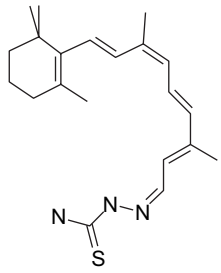

Scheme 1. Drawing of ligand Hret (**1**).

a spectroscopic investigation with calf thymus DNA has been carried out. A particularly important property necessary to evaluate for in vivo use is the logarithm of the experimental *n*-octanol/water partition coefficient ($\log P_{ow}$). This is an important pharmacological descriptor of bioavailability for both organic compounds and inorganic complexes [13]. Predicting and altering $\log P_{ow}$ is a key element in rational drug design since the correct incorporation of lipophilic groups in a chemical compound can result in an increase in biological activity [14]. With this aim partition coefficient for the ligand and its complexes were determined. The ligand and their complexes have been also tested in vitro on human leukemic cell line U937 to find those compounds that are able to inhibit cell proliferation with non-toxic effects for healthy cells and to evaluate their ability to induce apoptosis.

2. Results and discussion

Ligand Hret (**1**) was prepared as can be seen in Section 4 conveniently modifying the synthesis reported in the literature [15]. This ligand is potentially SN bidentate and it has a NH group deprotonatable as a function of pH. After purification, the yellow solid is air-stable, DMSO and EtOH soluble. The determined $\log P_{ow}$ is 1.05.

In agreement with the microanalytical data for the solid state, ESI-MS spectroscopy shows that the cationic $[Cu(ret)]^+$ (*m*/*z* 420) moiety with the NS bidentate ligand is the prevalent species in solution as expected for this class of systems [16].

Complex (**2**) $[Cu(ret)Cl(OH_2)]\cdot H_2O$, is represented in Fig. 1.

ESR absorption spectra of complex (**2**) were examined. Signals were detected in the room temperature to liquid nitrogen temperature region. Apart from the obvious variation of the intensity, the spectra remain qualitatively unchanged in the whole temperature range. The powder signal shows two extreme absorption peaks characterized by Landé factors $g_1 = 2.238$ and $g_2 = 2.045$ with evidence of an unresolved signal at intermediate g value. The measured g values are typical for a Cu(II) complex and may be explained assuming a square planar arrangement ($3d_{x^2-y^2}$ unpaired electron) with, possibly, some rhombic in-plane distortion. As a matter of fact the lack of structural data of the complex prevents a definite conclusion about the unpaired electron orbital, if $d_{x^2-y^2}$ or d_{z^2}. In spite of this, some reasons remain supporting the presence of an unpaired electron in the $d_{x^2-y^2}$ orbital: (1) the tetragonally distorted coordination is uncomparably the most usual one for a Cu^{2+}complex ion; (2) the observed values $g_1 = 2.238$ and $g_2 = 2.045$ seem quite close to values frequently found in copper complexes with a mean covalent character $\alpha^2 \sim 0.75$ and are roughly in line with the approximate ratio $(g_{\|} - 2)/(g_{\perp} - 2) \sim 4$ valid for a d^9 tetragonal ion in a intermediate ligand field situation [17]; (3) if two Cu^{2+} ions distinct in orientation are present in the unit cell, the observed values $g_1 = 2.238 \geq g_x(\text{not resolved}) > g_2 = 2.045$ may be easily explained in terms of exchange averaging of two elongated axial g factors with $g_{\perp} = 2.05$.

The $\log P_{ow}$ for Cu(II) complex is 1.09.

Complex (**3**) $[Co(Hret)_3]Cl_3\cdot 4H_2O$ was also isolated using Co(III) chloride salt. The same complex was obtained using a 1:2 stoichiometric ratio with respect to the ligand. The ESI-MS spectrum shows the presence of cationic coordinated moiety. The elemental analysis confirms the presence of the counterions while the NMR confirms that the ligand is not deprotonated. The NMR spectrum allows also to hypothesize to a pseudo octahedral low spin coordination geometry. The presence of different resonances assignable to C*H* retinal chain and C*H*N moiety is representative of the presence in solution of both Λ and Δ isomers together. The experimental $\log P_{ow}$ determined for Co(III) complex is 1.89.

Complex (**4**) $[Ni(ret)_2]\cdot 3H_2O$ shows a square planar S_2N_2 geometry. Both ligands are deprotonated as expected using acetate as metal counterion. The apparent octanol/water partition coefficients determined for Ni(II) complex is 1.37. The ^1H NMR spectrum is very simple and this reflects a high symmetry of the molecule due to a *trans* isomer as the prevalent (see Fig. 2).

2.1. Absorption spectral features of DNA binding

The binding constant obtained for ligand **1** is $8.3 \times 10^5\ M^{-1}$, while for complexes $[Cu(ret)Cl(OH_2)]\cdot H_2O$ (**2**),

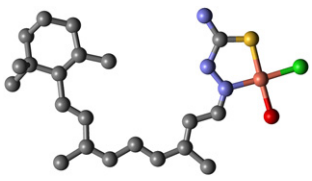

Fig. 1. Assumed structure of the coordinated moiety of complex (**2**) $[Cu(ret)Cl(OH_2)]$ (hydrogens omitted for clarity).

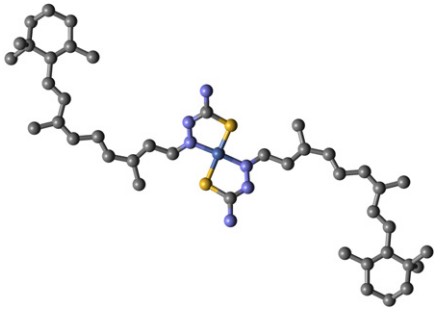

Fig. 2. Assumed structure of complex (**4**) $[Ni(ret)_2]$ (hydrogens omitted for clarity).

$[Co(Hret)_3]Cl_3 \cdot 4H_2O$ (**3**), and $[Ni(ret)_2] \cdot 3H_2O$ (**4**) are $5.8 \times 10^5\ M^{-1}$, $4.1 \times 10^4\ M^{-1}$, and $2.6 \times 10^6\ M^{-1}$, respectively (each experiment was performed in triplicate). In Fig. 3 is reported the plot of $[DNA]/(\varepsilon_A - \varepsilon_f)$ vs [CT-DNA] for absorption titration of the studied compounds, useful for obtaining K_b by the ratio of the slope to intercept.

Our experimental K_b values are of interest if compared with those observed for classical intercalators (ethidium–DNA, 1.4×10^6 in 25 mM Tris–HCl/40 mM NaCl buffer, pH = 7.9 [18]; 3.0×10^6 in 5 mM Tris–HCl/50 mM NaCl buffer, pH = 7.2 [12], indicating a different behavior of compounds towards DNA. Uncomplexed ligand (**1**) and its copper complex (**2**) bind DNA with less affinity than intercalators (even if strongly than what was previously found), as already observed and noticed for organic small molecules and copper(II) complexes with thiosemicarbazonato or macrocyclic ligands [12,20]. After coordination, no significant increase of K_b was observed for copper complex (**2**) with respect to the ligand probably meaning that the good constant value is related to the role played by the ligand in the binding to DNA. On the other hand, coordination of the ligand with the cobalt center in complex (**3**) leads to a decrease in the capacity of interaction towards DNA. The complete octahedral environment with such a bulky ligand is not suitable for a good match of the molecule with the nucleic acid. On the other hand the square planar nickel complex (**4**) showed an increased and remarkable value for K_b to the same magnitude order of intercalators ($10^6\ M^{-1}$). Hypochromism and red shift (bathochromism) in electronic absorption spectra of DNA bound to different compounds are generally attributed to intercalation, involving a strong stacking interaction between aromatic chromophores and the base pairs of DNA. In this work, these features were observed only for compound **4** (see Fig. 4), and the spectra are different from those for ligand **1** and its complexes **2** and **3** that instead are fairly similar.

The ratio r ($r = [CT\text{-}DNA]/[complex]$) varied between 0.2 and 1 in 5 mM Tris–HCl buffer (pH = 7.2), 50 mM NaCl at 25 °C. The arrow at ca. 260 nm indicates the direction of absorbance changes as a function of increasing r. As expected for bound compounds, the typical DNA absorption decreases when [complex] increases. On the other hand the maximum absorption at the studied wavelength (424 nm) is reached for

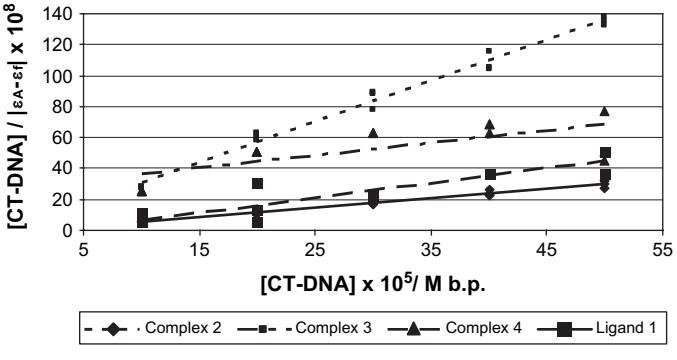

Fig. 3. Typical plots of plot $[DNA]/(\varepsilon_A - \varepsilon_f)$ vs [CT-DNA] for absorption titration with CT-DNA in 50 mM NaCl/5 mM Tris buffer, pH 7.2 at 25 °C.

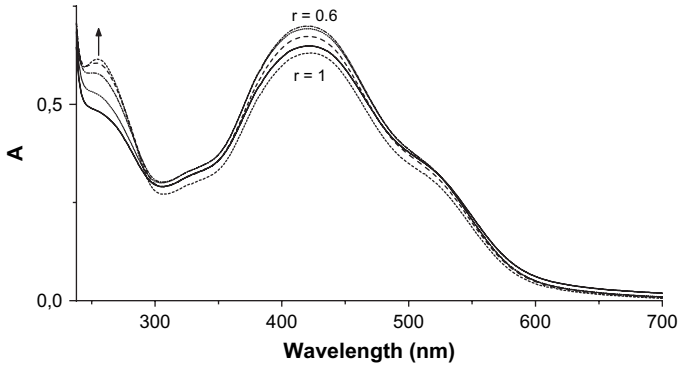

Fig. 4. Variation in absorption spectrum of complex $[Ni(ret)_2] \cdot 3H_2O$ (**4**) 20 μM with increasing amount of CT-DNA.

$r = 0.6$. This value probably represents for the complex the best ratio for an intercalative behavior. For ligand **1**, the different spectroscopic behavior can be explained as the dissociation of ligand aggregates, which is already seen for other aromatic ligands [21]. A similar hyperchromism was observed also for a Cu(II) complex with a ligand bearing NH and OH groups [19] and for the Soret bands of certain porphyrins showing interactions with DNA [22]. This feature has not yet been well explained. We think that the difference in the absorption spectral behavior is due to the possibility for **1** and **2** to have more hydrogen bonding interactions, in agreement with Ref. [19] while for compound **3**, the complex polyhedron does not fit with DNA. A more classical behavior for nickel complex **4** is probably due to its increased hydrophobicity; in addition, the electronic spectrum of the adduct of **4** with DNA shows the presence of a shoulder (at ca. 530 nm) not visible in the spectra of other compounds, which highlights different behavior and suggests the presence of a new molecular species responsible for interactions.

Nevertheless, even for compounds **1** and **2** a partial intercalation cannot be excluded to explain the K_b values, or an external mode of binding to DNA leading to modest electronic coupling with the host could be considered, as already noted for Cu(II) complexes [21].

2.2. Partition coefficient evaluation

The experimental apparent octanol/water partition coefficient $\log P_{ow}$ values increase as the number of ligand unit per metal unit increases, finally the maximum of lipophilicity for cobalt complex (**3**) was found. It could surprise to find an enhanced lipophilicity for the trication (**3**) compared with the neutral species (**2**) and (**4**) with the same ligand; but it is necessary to consider that the comparison is made amongst non-homologous series. In fact the partition of ions between octanol and water is a much more complex process than that of neutral species. The observed concentration ratio for the ions is related not only to the partition of the ion but also to the partition of the ion pair [23]. It is believed that the higher $\log P_{ow}$, i.e., the more lipophilic the molecule, the faster the molecule crosses the intestinal barrier in the case of intestinal absorption for the drug delivery [24]. Generally, compounds

with $\log P_{ow}$ values less than 1.5 tend to exhibit minimal distribution into lipid membranes while compounds ranging between 2 and 4 tend to exhibit excellent partitioning in membranes [25,26]. In our study cobalt complex could exhibit the best absorption by the organic membrane, but the best biological activity will be exhibited by the copper compounds with $\log P_{ow}$ value at ca. 1.

2.3. Effects on cell proliferation and apoptosis induction

Ligand (**1**) and its complexes (**2**), (**3**) and (**4**) were evaluated in vitro for their cytotoxicities, using peripheral blood mononuclear cells (PBMC) as a control, against cell line U937. The compounds showed no effect on PBMC also at rather high concentrations. The synthesized compounds were therefore tested on human leukemic cell line U937 in order to evaluate their capability to induce cell proliferation inhibition and apoptosis.

In Figs. 5–7 are represented the effects on cell growth at different time steps of complexes $[Cu(ret)Cl(OH_2)]\cdot H_2O$ (**2**), $[Co(Hret)_3]Cl_3$ (**3**) and $[Ni(ret)_2]\cdot 3H_2O$ (**4**), respectively.

Ligand Hret did not show a significant antiproliferative activity at least at a non-toxic concentration.

Copper complex (**2**) exhibited a relevant biological activity already after 24 h of treatment at an IC_{50} of 14.8 μM. Cobalt complex (**3**) did not show an interesting biological activity up to a concentration of ca. 18 μM. At the tested concentration of 22.2 μM the complex exerted a good inhibition of cell proliferation on the second day but on the third day it completely stopped cell growth (see Fig. 6).

Also for nickel complex (**4**) no activity was observed up to a concentration of ca. 26 μM, and for a concentration of about 30 μM the cytotoxic effect was prevalent with respect to cell proliferation inhibition effect, stopping the growth of cells (see Fig. 7).

We have carried out a blank assay using a concentration of inorganic salt in the same range of IC_{50} but we observed no effect on cell proliferation.

Due to the significant and interesting antiproliferative activity, complex (**2**) was also evaluated to verify its capability to induce apoptosis. At the IC_{50} value of 14.8 μM already after 24 h it exhibited ca. 13% of cells in early stages of apoptosis and ca. 42% in later stages (see Fig. 8); after 48 h ca. 98% of cells were in later stages of apoptosis.

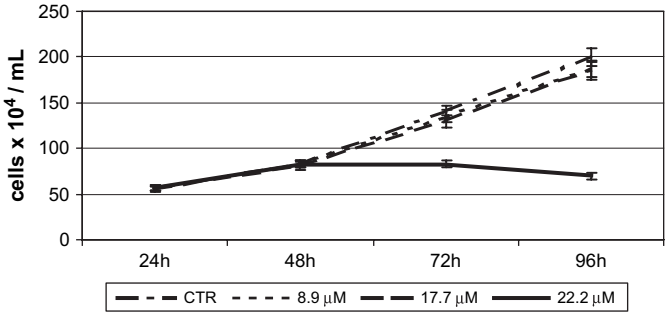

Fig. 6. Effects on U937 proliferation day per day following addition of $[Co(Hret)_3]Cl_3$ (**3**) at reported concentrations. Experiments were performed in quintuplicate and the control (CTR) contains the maximum concentration of DMSO used to dissolve the complex.

Log β of metal complexes of SN bidentate ligands in very closely related systems falls in the range from 6 to 12 [27,28]. With these assumption, log of formation constant for the complexes described in this paper can be supposed to be of about 10, consequently free metal ion concentration in the culture medium can be, in the worst hypothesis, ca. 10^{-8} M.

3. Conclusions

The synthesis and characterization of a new retinoid derivative have been carried out together with its Cu(II), Ni(II) and Co(III) complexes. The ligand binds quite strongly to DNA by an external mode; a similar feature is observed by its square planar Cu(II) complex probably again because of the presence of the retinoid moiety. The Co(III) octahedral complex has no interaction with the nucleic acid probably because of its bulky environment that does not fit well with DNA spaces. The square planar Ni(II) complex shows a very strong interaction with DNA probably due to intercalation. By partition coefficient measurements the higher lipophilicity is observed for cobalt complex. From proliferation inhibition and apoptosis

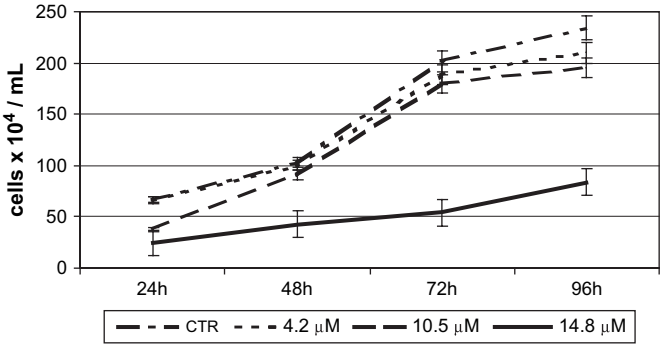

Fig. 5. Effects on U937 proliferation day per day following addition of $[Cu(ret)Cl(OH_2)]\cdot H_2O$ (**2**) at reported concentrations. Experiments were performed in quintuplicate and the control (CTR) contains the maximum concentration of DMSO used to dissolve the complex.

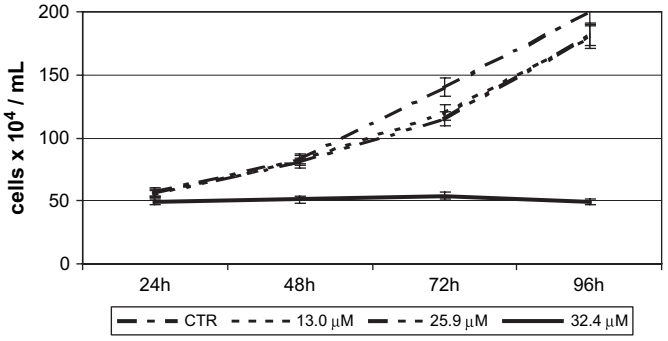

Fig. 7. Effects on U937 proliferation day per day following addition of $[Ni(ret)_2]\cdot 3H_2O$ (**4**) at reported concentrations. Experiments were performed in quintuplicate and the control (CTR) contains the maximum concentration of DMSO used to dissolve the complex.

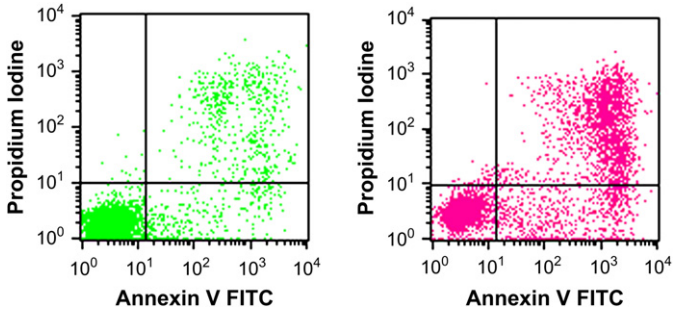

Fig. 8. Quantification of apoptosis for U937 cells treated with complex [Cu(ret)Cl(OH_2)]·H_2O (**2**) (right) and DMSO as control (left) performed by staining apoptotic cells with Annexin V-FITC and propidium iodide. Dot plots refer to the percentage of cells undergoing early stages of apoptosis (lower right quadrant: 12.7% for cells treated with complex) and later stages of apoptosis (upper right quadrant: 41.64% for cells treated with complex).

induction studies this class of compounds is really promising. The metal complexes show an increased activity if compared to the activity of the ligand alone. Cu(II) complex in particular has an IC_{50} in the micromolar range and it is able to induce apoptosis already at early stages. The IC_{50} of our compounds (ca. 10 μM) on the same cell line is of the same magnitude order, highlighting an effect comparable to compounds such as CDDP but with a less cytotoxic metal.

4. Experimental protocols

4.1. Physical measurements and general procedures

9-*cis*-Retinal, 98% purchased from Aldrich Chem. Co., thiosemicarbazide purchased from Jannsen, $CuCl_2·2H_2O$, $CoCl_2·6H_2O$, and $Ni(CH_3COO)_2·4H_2O$ from Carlo Erba were used as received.

All solvents are commercially available and were used as received except Et_2O, which was distilled over Na. The ^1H NMR spectra were recorded on a Bruker 300 spectrometer. Chemical shifts are reported in parts per million referenced to that of residual solvent protons. Infrared spectra were recorded as KBr pellets from 4000 to 400 cm^{-1} on a Perkin–Elmer FT-IR Nexus spectrometer. Elemental analyses (C, H, N, S) were performed with a Carlo Erba EA 1 108 automated analyzer. Mass spectra for the ligand were run on a Finnigan 1020 spectrometer (CI). ESR absorption spectra were recorded by a Varian E-line EPR spectrometer operating at the X-band with a 100 KHz field modulation. Magnetic fields were measured by use of a DPPH marker. Melting points were determined with a Gallenkamp instrument. UV measurements were performed on a Perkin–Elmer UV–vis Lambda 25 spectrometer with quartz cuvettes.

Calf thymus (CT) DNA was obtained from Serva and used as received. DNA samples were dissolved in 50 mM NaCl/5 mM Tris, pH 7.2. A solution of CT-DNA (ca. 10^{-5} M in base-pair, [bp]) in this buffer gave ratios of UV absorbance at 260 and 280 nm, A_{260}/A_{280}, of ca. 1.8, indicating that the CT-DNA was sufficiently free of protein. The concentration of the nucleic acid solutions was determined by UV absorbance at 260 nm after 1:100 dilution. The extinction coefficient ε_{260} was taken as 13 100 $M^{-1}\,cm^{-1}$ [29]. Stock solutions were stored at 4 °C and used after not more than four days.

4.2. Electrospray-mass spectroscopy

Metal complexes dissolved in CH_3CN were characterized by means of ESI-MS. A Quattro LC (Micromass, Manchester, U.K.) triple quadrupole instrument equipped with a pneumatically assisted electrospray ionization interface was used. An NT workstation with MassLynx v3.4 software was used for data acquisition and processing. In the ESI experiments the nebulizer gas (nitrogen, 99.999% purity) and the desolvation gas were delivered at flow rates of 111 and 596 L/h, respectively. The direct infusion mode operating with a Harvard syringe pump (Quebec, Canada) at a flow rate of 7 μL/min was used to optimize the ESI interface parameters on the MS response of the compounds. ESI-MS measurements were performed in positive ion (PI) mode. Interface parameters were set as follows: capillary voltage 3 kV, cone voltage 50 V, extractor lens 2 V, source temperature 70 °C, desolvation temperature 70 °C, RF lens 0.2 V. Quadrupoles were tuned to unit resolution. Full-scan mass spectra were acquired over the *m/z* 50–1800 scan range using a step size of *m/z* 0.1 and a scan time of 2.0 s with an interscan delay of 0.01 s.

4.3. Preparation of Hret (*1*)

In a 100 mL round-bottomed flask, thiosemicarbazide (31.6 mg, 0.345 mmol) was suspended in absolute diethyl ether prepared as previously described (60 mL) in the presence of molecular sieves (3 Å) and under N_2 flux. The flask was placed in the dark in an ice bath and the mixture was stirred until cooling. 9-*cis*-Retinal (100 mg, 0.345 mmol) was then added directly in the flask and the mixture was kept cold and stirred in the dark for 4 days. The obtained mixture was then filtered under vacuum using a blue ribbon filtering paper. The product was allowed to crystallize from its yellow solution at 0 °C and a shiny yellow powder was isolated (100.1 mg, 81%). Mp: 98.8 °C. CI-MS (*m/z*, rel intens): 357, 100 (M^+). ^1H NMR ($CDCl_3$): δ 1.07 (s, $2CH_3$, ring), 1.45 (m, CH_2), 1.57 (m, $2CH_2$), 1.67 (m, CH_3, ring), 1.94 (bs, $2CH_3$, chain), 6.12 (s, CH, chain), 6.21 (s, CH, chain), 6.34 (t, CH, chain), 6.73 (s, CH, chain), 6.84 (s, CH, chain), 6.92 (bs, NH_2), 7.13 (dd, CH, chain), 7.33 (d, CHN). IR (KBr pellets, cm^{-1}): 3422, 3262, 2927, 1653, 1030, 668. Anal. Calcd for $C_{21}H_{31}N_3S$: C, 70.59; H, 8.68; N, 11.76; S, 8.98%. Found: C, 71.01; H, 8.56; N, 11.96; S, 8.75.

4.4. Preparation of [Cu(ret)Cl(OH_2)]·H_2O (*2*)

In a 100 mL round-bottomed flask, Hret (**1**) (112 mg, 0.314 mmol) was dissolved at room temperature in 96% EtOH (50 mL). The solution was dark yellow. An equimolar amount of $CuCl_2·2H_2O$ (54 mg, 0.314 mmol) was dissolved in 96% EtOH (15 mL) and added dropwise to the solution

of the ligand magnetically stirred. The resulting solution became red. After 30 min stirring the solution was allowed to crystallize. A deep red powder was found after solvent evaporation. The obtained product was then purified by re-crystallization from a solution of *i*-propyl alcohol:ethanol = 1:2 (107.7 mg, 70%). Mp: 150.5 °C (dec). ESI-MS (*m/z*, rel intens): 420, 100 $[Cu(ret)]^+$. IR (KBr pellets, cm^{-1}): 3420, 3262, 3147, 2927, 2862, 1605, 1572, 1026, 962. Anal. Calcd for $C_{21}H_{34}N_3O_2SCuCl$: C, 51.32; H, 6.97; N, 8.55; S, 6.52%. Found: C, 51.42; H, 7.01; N, 8.65; S, 6.49.

4.5. Preparation of $[Co(Hret)_3]Cl_3 \cdot 4H_2O$ (**3**)

In a 100 mL round-bottomed flask, Hret (**1**) (235 mg, 0.658 mmol) was dissolved at room temperature in 96% EtOH (50 mL). The solution was dark yellow. $CoCl_2 \cdot 6H_2O$ in a 1:3 molar ratio with respect to the ligand (52 mg, 0.219 mmol) was dissolved in 96% EtOH (20 mL) and added dropwise to the solution of the ligand magnetically stirred. The resulting solution became dark brown. After 6 h stirring the solution was allowed to crystallize. A dark brown powder was found after solvent evaporation. The obtained product was then purified by re-crystallization from a solution of *i*-propyl alcohol:ethanol = 1:2 (157.6 mg, 55%). Mp: 282.8 °C. ESI-MS (*m/z*, rel intens): 377, 50 1/3$[Co(Hret)_3]^{3+}$, 583, 40 1/2$\{[Co(Hret)_3]Cl\}^{2+}$. ^1H NMR ($CDCl_3$): δ 1.12 (s, $2CH_3$, ring), 1.34 (m, CH_2), 1.48 (m, $2CH_2$), 1.69 (m, CH_3, ring), 2.01 (bs, $2CH_3$, chain), 6.14 (s, CH, chain), 6.20 (s, CH, chain), 6.32 (t, CH, chain), 6.63 (s, CH, chain), 6.88 (s, CH, chain), 6.90 (bs, NH_2), 7.13–7.23 (dd, CH, chain), 7.33–7.45 (d, CHN). IR (KBr pellets, cm^{-1}): 3520, 3410, 3128, 2925, 2882, 1615, 1584, 1025, 895. Anal. Calcd for $C_{63}H_{101}N_9O_4S_3CoCl_3$: C, 57.77; H, 7.77; N, 9.62; S, 7.34%. Found: C, 57.82; H, 8.05; N, 9.98; S, 7.02.

4.6. Preparation of $[Ni(ret)_2] \cdot 3H_2O$ (**4**)

In a 100 mL round-bottomed flask, Hret (**1**) (185 mg, 0.518 mmol) was dissolved at room temperature in 96% EtOH (45 mL). The solution was dark yellow. $Ni(CH_3COO)_2 \cdot 4H_2O$ in a 1:2 molar ratio with respect to the ligand (74 mg, 0.259 mmol) was suspended in 96% EtOH (5 mL) and added dropwise to the solution of the ligand magnetically stirred. The resulting solution became deep red. After 1 h stirring the formation of powder was observed and the solution was filtered with the aid of a buchner. The solution was then allowed to crystallize. The obtained product was then washed with EtOH many times (180 mg, 84%). Mp: 175.5 °C. ESI-MS (*m/z*, rel intens): 772, 100 $[Ni(Hret)(ret)]^+$. ^1H NMR (DMSO-d_6): δ 1.00 (s, $2CH_3$, ring), 1.45 (m, CH_2), 1.57 (m, CH_2), 1.68 (m, CH_3, ring), 1.94 (d, $2CH_3$, chain), 2.02 (m, CH_2), 6.12 (s, CH, chain), 6.16 (s, CH, chain), 6.27 (t, CH, chain), 6.70 (s, CH, chain), 6.75 (s, CH, chain), 6.91 (bs, NH_2), 7.05 (dd, CH, chain), 7.30 (d, CHN). IR (KBr pellets, cm^{-1}): 3510, 3400, 3145, 2935, 2892, 1612, 1580, 1015, 875. Anal. Calcd for $C_{42}H_{66}N_6O_3S_2Ni$: C, 61.16; H, 8.07; N, 10.19; S, 7.77%. Found: C, 61.70; H, 8.07; N, 9.89; S, 7.23.

4.7. DNA interaction studies

The interaction between the compounds under study and DNA was determined by binding constants as already described [30]. The intrinsic binding constant K_b for the interaction of the ligand and its complexes with CT-DNA was calculated by absorption spectral titration data using the equation $1/\Delta\varepsilon_{ap} = 1/(\Delta\varepsilon K_b D) + 1/\Delta\varepsilon$ where $\Delta\varepsilon_{ap} = |\varepsilon_A - \varepsilon_f|$, $\Delta\varepsilon = |\varepsilon_B - \varepsilon_f|$, D = [DNA], and ε_A, ε_B, and ε_f are the apparent, bound, and free extinction coefficients of the compound, respectively. K_b is given by the ratio of the slope to intercept when it is reported in the plot of [DNA]/($\varepsilon_A - \varepsilon_f$) vs [DNA] and is expressed as M^{-1}. The mentioned equation was originally used to calculate the binding constants for hydrophobic derivatives; nowadays it is broadly used to investigate a wide variety of metal complexes containing phenanthroline and its derivatives and, recently, has been adopted to obtain binding constant values from metal complexes with different ligands [12,19,20,31,32]. Established amounts of the ligand and of the complexes were dissolved in DMSO because the high solubility in this solvent allows us to prepare concentrated solutions and therefore to utilize reduced volumes (5 μL) for titrations. It was also verified that the DMSO percentage (0.7%) added to the DNA solution did not interfere with the nucleic acid; in fact, the 260 nm absorption band is not subjected to modifications in intensity and position. Concentrated solutions of NaCl, Tris–HCl (pH 7.2) buffer, and DNA were prepared. Calculated amounts of the described stock solutions were taken to final concentration values of 50 mM NaCl, 5 mM Tris–HCl, and increasing amounts of DNA over a range of DNA concentrations from 10^{-5} to 10^{-3} M. These solutions were then added to the 5 μL solution of the considered compound in order to maintain the final volume of the solutions fixed to 700 μL. The compounds were titrated at room temperature. The changes in absorbance of DNA of an absorption band upon each addition were monitored at the maximum wavelengths 380, 364, 396 and 424 nm for **1**, **2**, **3** and **4**, respectively.

4.8. Partition coefficient determination

The apparent octanol/water partition coefficients ($\log P_{ow}$) were determined using 50 mM NaCl/5 mM Tris, pH 7.2 buffer as the water phase. Briefly, the octanol was pre-saturated with the buffer for more than 24 h before use. A 24.8 μL aliquot of each compound (of known pre-evaluated concentration), dissolved in octanol, was added to three different ratios of octanol/water buffer for a total volume of 3 mL. The samples were placed on a shaker for 6 h at 37 °C. After shaking, the samples were centrifuged for 5 min at 13 000×*g* on a table-top microcentrifuge. The organic and the water phase were then analyzed by means of UV-spectrometry in order to determine the concentration of the examined compound in each of them. The ratio of concentrations in octanol vs buffered water phase was determined for each sample. The ratios were then

averaged for the three different octanol/water buffer's ratios used for each compound to calculate the partition coefficient.

4.9. Biological data. Cell culture

U937, a monoblastoid line, was obtained from American Type Culture Collection (ATCC, Rockville, MD) and cultured in RPMI 1640 medium (Gibco BRL, Life Technologies Italia, Milano) supplemented with 10% (v/v) fetal bovine serum (FBS) (Hyclone Europe, Cramlington, UK), 100 units/mL penicillin, 100 μg/mL streptomycin, and 2 mM L-glutamine at 37 °C and in a humidified atmosphere containing 5% CO_2.

PBMC used for the control were purified from 10 healthy subjects by density gradient centrifugation on a Ficoll/sodium diatrizoate solution (Nycomed Pharma As, Oslo, Norway). PBMCs, were cultured in RPMI 1640 medium, supplemented with 10% FBS, in the absence or in the presence of rIL-2 (20 U/mL) and phytohemaglutinin (PHA) at 1 μg/mL for 72 h before treatment with compounds.

4.10. Viability and proliferation assays

Cell lines or PBMCs were plated at 1×10^5/mL and 2×10^5/mL, respectively, in 96-well plates in the presence of increasing concentrations of compounds. IC_{50} are evaluated after 24 and 48 h of culture by ProCheck cell viability assay (Intergen Canada) and was performed according to the manufacturer protocol. The cell viability assay is based on the conversion of XTT (sodium 3,3′-{1-[(phenylamino)carbonyl]-3, 4-tetrazolium}bis(4-methoxy-6-nitro)benzenesulfonic acid) from an oxidized tetrazole to a reduced formazan and on the direct spectrophotometric detection of the colored product in the reaction well. The orange-red formazan has an absorbance maximum at 475 nm. Test cells are dispensed in a volume of 100 μL into microtiter wells in medium that does not contain reducing agents, add 20 μL of ProCheck™ cell viability reagent to the cell samples in the well for a total volume of 120 μL. The cells are incubated under growth conditions, protected from light for 1–4 h, until sufficient color is present to read the optical density at 475 ± 25 nm in a microplate spectrophotometer. Cells in the exponential phase of growth were seeded in duplicate in 30 mm tissue culture dishes. After seeding (24 h), exponentially proliferating cells were treated with the compounds and the cells were incubated for 48 h. The cell number was counted after 24–48 h of incubation (continuous exposure assay) using a hematocytometer by trypan blue staining.

4.11. Apoptotic assay

For apoptosis determination the MBL MEBCYTO® Apoptosis Kit Annexin V Assay was used, this can better identify cells in an earlier stage of apoptosis than assays based on DNA fragmentation. Staining the cells with Annexin V-FITC and propidium iodide (PI) can be used in a bivariate analysis to distinguish between cells undergoing apoptosis (PI negative) and those that are necrotic or dead (PI positive). Cells (2×10^5) were incubated with FITC-labeled Annexin V and propidium iodide (PI) at room temperature for 15 min in the dark and analyzed using a FACSCalibur (Beckton–Dickinson).

Acknowledgments

This work was supported by the Ministero dell'Istruzione Università e Ricerca of Italy (MIUR, PRIN.2004059078_004). The authors thank C.I.R.C.M.S.B (Consorzio Interuniversitario di Ricerca in Chimica dei Metalli nei Sistemi Biologici).

References

[1] L. Feun, M. Modiano, K. Lee, J. Mao, A. Marini, N. Savaraj, P. Plezia, B. Almassian, E. Col acino, J. Fischer, S. MacDonald, Cancer Chemother. Pharmacol. 50 (2002) 223–229.
[2] D.B. Lovejoy, D.R. Richardson, Blood 100 (2002) 666–676.
[3] L.-J. Ming, Med. Res. Rev. 23 (2003) 697–762.
[4] C.A. Barker, W.E. Burgan, D.J. Carter, K. Camphausen, P.J. Tofilon, Int. J. Radiat. Oncol. Biol. Phys. 63 (2005) S170.
[5] P. Wolohan, J. Yoo, M.J. Welch, D.E. Reichert, J. Med. Chem. 48 (2005) 5561–5569.
[6] P. Tarasconi, S. Capacchi, G. Pelosi, M. Cornia, R. Alberini, A. Bonati, P.-P. Dall'Aglio, P. Lunghi, S. Pinelli, Bioorg. Med. Chem. 8 (2000) 157–162.
[7] M. Belicchi-Ferrari, F. Bisceglie, G. Pelosi, M. Sassi, P. Tarasconi, M. Cornia, S. Capacchi, R. Alberini, S. Pinelli, J. Inorg. Biochem. 90 (2002) 113–126.
[8] J.S. Bertram, A.L. Vine, Biochim. Biophys. Acta – Mol. Basis Dis. 1740 (2005) 170–178.
[9] K. Melancon, Q. Cheng, T.L. Kiefer, J. Dai, L. Lai, C. Dong, L. Yuan, A. Collins, A. Thiyagarajah, S. Long, S.M. Hill, Cancer Lett. 227 (2005) 39–48.
[10] W. Smith, N. Saba, Crit. Rev. Oncol. Hematol. 55 (2005) 143–152.
[11] P. Zhang, Q. Xu, W.-T. Chen, L.-Q. Duan, Z.-Y. Zhang, X.-J. Zhou, Oral Oncol. 41 (2005) 909–915.
[12] M. Baldini, M. Belicchi-Ferrari, F. Bisceglie, G. Pelosi, S. Pinelli, P. Tarasconi, Inorg. Chem. 42 (2003) 2049–2055.
[13] C.A. Lipinski, F. Lombardo, B.W. Dominy, P.J. Feeney, Adv. Drug Deliv. Rev. 23 (1997) 3–25.
[14] P.R. Andrews, D.J. Craik, J.L. Martin, J. Med. Chem. 27 (1984) 1648–1657.
[15] V. Buss, K. Kolster, B. Görs, Tetrahedron 4 (1993) 1–4.
[16] O.E. Offiong, Transition Met. Chem. 23 (1998) 553–555.
[17] A. Abragam, B. Bleaney, Electron Paramagnetic Resonance of Transition Ions, Clarendon Press, Oxford, 1970.
[18] W.D. Wilson, F.A. Tanious, M. Fernandez-Saiz, C.T. Rigl, in: K.R. Fox (Ed.), Methods in Molecular Biology, vol. 90, Humana, Clifton, NJ, 1997.
[19] J. Liu, T. Zhang, T. Lu, L. Qu, H. Zhou, Q. Zhang, L. Ji, J. Inorg. Biochem. 91 (2002) 269–276.
[20] M. Baldini, M. Belicchi-Ferrari, F. Bisceglie, P.-P. Dall'Aglio, G. Pelosi, S. Pinelli, P. Tarasconi, Inorg. Chem. 43 (2004) 7170–7179.
[21] F. Liu, K.A. Meadows, D.R. McMillin, J. Am. Chem. Soc. 115 (1993) 6699–6704.
[22] R.F. Pasternack, E.J. Gibbs, J.J. Villafranca, Biochemistry 22 (1983) 2406–2412.
[23] Y.H. Zhao, M.H. Abraham, J. Org. Chem. 70 (2005) 2633–2640.
[24] W. Rubas, M.E.M. Cromwell, Adv. Drug Deliv. Rev. 23 (1997) 157–162.
[25] A. Martin, Physical Pharmacy – Physical Chemical Principles in the Pharmaceutical Sciences, Lea and Febiger, Philadelphia, 1993 pp. 237–241.

[26] M. Martinez, L. Augsburger, T. Johnston, W. Warren Jones, Adv. Drug Deliv. Rev. 54 (2002) 805–824.
[27] F. Dallavalle, F. Gaccioli, R. Franchi-Gazzola, M. Lanfranchi, L. Marchiò, M.A. Pellinghelli, M. Tegoni, J. Inorg. Biochem. 99 (2002) 95–104.
[28] F. Gaccioli, R. Franchi-Gazzola, M. Lanfranchi, L. Marchiò, G. Metta, M.A. Pellinghelli, S. Tardito, M. Tegoni, J. Inorg. Biochem. 99 (2005) 1573–1584.
[29] M.E. Reichmann, S.A. Rice, C.A. Thomas, P. Doty, J. Am. Chem. Soc. 76 (1954) 3047–3051.
[30] A. Wolfe, G.H. Shimer Jr., T. Meehan, Biochemistry 26 (1987) 6392–6396.
[31] Mudasir, N. Yoshioka, H. Inoue, J. Inorg. Biochem. 77 (1999) 239–247.
[32] M. Baldini, M. Belicchi-Ferrari, F. Bisceglie, S. Capacchi, G. Pelosi, S. Pinelli, P. Tarasconi, J. Inorg. Biochem. 99 (2005) 1504–1513.